Available online at www.sciencedirect.com
ScienceDirect
C. R. Physique 8 (2007) 123–137
COMPTES RENDUS PHYSIQUE
http://france.elsevier.com/direct/COMREN/

Recent advances in crystal optics/Avancées récentes en optique cristalline

Optical waveguides in laser crystals

Markus Pollnau [a,b,*], Yaroslav E. Romanyuk [a]

[a] *Advanced Photonics Laboratory, Institute of Imaging and Applied Optics, École Polytechnique Fédérale de Lausanne, CH-1015 Lausanne, Switzerland*

[b] *MESA+ Institute for Nanotechnology, University of Twente, P.O. Box 217, NL-7500 AE Enschede, The Netherlands*

Available online 8 August 2006

Invited Paper

Abstract

This article reviews the recent research on different types of planar and channel crystalline optical waveguides, fabrication methods such as liquid phase epitaxy, pulsed laser deposition, thermal bonding, reactive ion or ion beam etching, wet chemical etching, ion in-diffusion, proton exchange, ion beam implantation, and femtosecond laser writing, as well as waveguide laser operation of rare-earth and transition-metal ions in oxide crystalline materials such as Al_2O_3, $Y_3Al_5O_{12}$, $YAlO_3$, $KY(WO_4)_2$, and $LiNbO_3$. ***To cite this article: M. Pollnau, Y.E. Romanyuk, C. R. Physique 8 (2007).***

Résumé

Guides d'ondes optiques en cristaux laser. Cet article fait le point sur les recherches récentes sur différents types de guides d'ondes optiques cristallins plans et canaux, ainsi que sur leurs méthodes de fabrication, comme l'épitaxie en phase liquide, la déposition par laser pulsé, le thermocollage, l'attaque par ions réactifs ou faisceau ionique, l'attaque chimique humide, la diffusion ionique, l'échange de protons, l'implantation par faisceau ionique, et la gravure par laser femtoseconde, ou encore le dopage laser de guides d'ondes par des ions de terres rares et de métaux de transition dans des oxydes cristallins tels que Al_2O_3, $Y_3Al_5O_{12}$, $YAlO_3$, $KY(WO_4)_2$ et $LiNbO_3$. ***Pour citer cet article : M. Pollnau, Y.E. Romanyuk, C. R. Physique 8 (2007).***

Keywords: Optical waveguides; Laser crystals

Mots-clés : Guides d'ondes optiques ; Cristaux laser

1. Introduction

In the past fifteen years, the field of integrated optics has made remarkable progress. The standard material for integrated optical devices is silicon. SiO_2 and Si_xN_y can be combined with silicon and have been employed in integrated optics. While these classes of materials offer advantages for precise etching of sub-micrometer structures, attempts to achieve high optical gain have not led to satisfactory results. In contrast, III–V semiconductors produce high optical gain at various wavelengths, especially in the region 630–980 nm. The main disadvantages are the com-

* Corresponding author.
E-mail address: m.pollnau@ewi.utwente.nl (M. Pollnau).

1631-0705/$ – see front matter
doi:10.1016/j.crhy.2006.04.002

plicated multi-layer growth by molecular beam epitaxy, the difficulties in combining these materials with silicon, and the relatively low threshold for optical damage, restricting the output power in a single optical mode to typically less than a Watt.

Alternatively, high optical gain and output power can be obtained in rare-earth or transition-metal ion doped dielectric materials. Although especially crystalline structures cannot be combined with silicon-based materials, these robust materials offer high optical damage thresholds. As miniaturized waveguide lasers and amplifiers, these systems will find applications whenever there is a need for on-chip optical gain in combination with high optical power, wavelength diversity, ultra-short pulses, or second- and third-order optical nonlinearities which can be exploited in order to integrate various optical functions on a chip.

In recent years, several fabrication methods have been investigated and various crystalline waveguide lasers could be demonstrated. In the following section, the principle waveguide structures will be described. Section 3 reviews those fabrication methods which require the deposition of a crystalline layer, followed by Section 4 about surface structuring. Waveguide fabrication methods which modify directly the bulk refractive index, thereby avoiding any layer deposition, are the subject of Section 5. In Section 6, recent examples of waveguide lasers in rare-earth and transition-metal ion doped oxide crystalline materials are presented.

2. Waveguide structures and laser geometries

In free-space propagation, a focused light beam exhibits a natural divergence after the focus. Optical waveguides inhibit this natural divergence. They possess a tailored refractive-index profile which leads to repeated total internal reflection of the light on its propagation path. In this way, the propagating light is confined in one or both lateral directions to a guiding region, thereby maintaining its high intensity. If the confinement is solely in the vertical direction, the waveguide structure is called two-dimensional or planar, whereas with additional horizontal confinement we obtain a one-dimensional, linear, or channel waveguide.

Larger refractive-index steps lead to higher acceptance angles for total internal reflection, which result in either a larger number of optical modes supported by the same waveguide cross-section or a smaller waveguide cross-section for the same optical mode profile, i.e., in higher optical intensities. On the other hand, scattering losses at the lateral optical interfaces increase with increasing refractive-index step. These features mark the typical differences between surface waveguides, which usually possess a high refractive-index step between the waveguide material and air, and buried waveguides, in which the waveguide region is laterally surrounded by material of often only slightly decreased refractive index.

Optical confinement can be achieved by a material of lower refractive index, which is thick compared to the penetration depth of the evanescent field of guided modes into the surrounding area, thereby establishing a refractive-index step. In contrast, if the region of lower refractive index is comparable to the depth of the evanescent field, while the laterally following region has similar or even higher refractive index compared to the waveguide, a refractive-index barrier is formed. The guided light can tunnel through this barrier and radiate laterally, which may lead to significant additional propagation losses.

Fig. 1 gives an overview of typical combinations of planar or channel, surface or buried, refractive-index step or barrier waveguides. In the following two sections, we will review the fabrication methods which can be employed to produce these different waveguide structures in crystalline dielectric materials.

Nowadays, most solid-state lasers are pumped by semiconductor laser diodes, arrays, or stacks, because of their high electrical-to-optical efficiency as well as narrow spectral linewidth, hence higher absorption coefficient when tuning to an absorption line of the active ions as compared to flashlamp pumping. Coupling of diode-laser pump light into waveguide structures can be performed in different ways. While fundamental-mode channel waveguides typically require end-face pumping by—also fundamental-mode—laser diodes, planar waveguide structures can also be side-pumped by diode bars or even top-pumped by diode stacks, provided that the layer is thick enough and the absorption coefficient high enough to ensure sufficient pump light absorption. These three pump schemes are depicted in Fig. 2.

Like in fiber lasers, also waveguide geometries which employ pump cladding layers with large refractive-index step above and below a core layer with low refractive index step have been explored. Such pump-cladding structures allow for end-pumping of the fundamental-mode waveguide core with low-brightness diode bars or stacks whose output is coupled into the cladding structure. In order to increase the thickness of the doped core layer, thereby improving pump absorption over the typically rather short waveguide length, while maintaining fundamental-mode output from the core

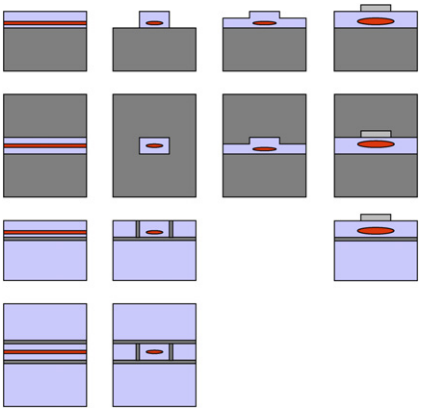

Fig. 1. Various types of planar or channel, surface or buried, refractive-index step or barrier waveguide geometries and indicated mode profiles of light guided in these structures.

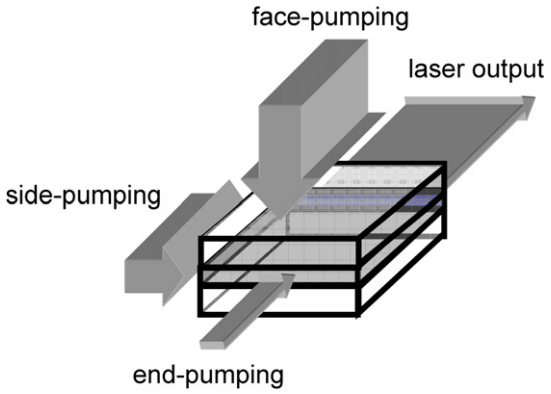

Fig. 2. Different coupling geometries for diode-laser pumping of waveguides.

layer, also large-mode-area structures with ultra-low refractive index difference between core and pump cladding can be employed, again following the same idea as in fiber lasers.

3. Planar waveguide fabrication by layer deposition

Two fundamentally different ways to obtain optical waveguides can be pursued. The first, which will be reviewed in this section, is based on the deposition of material as a thin crystalline layer on a substrate. The difference in refractive index between layer and substrate is obtained by doping either the layer itself—in the majority of cases by the optically active ions—or the substrate. Alternatively, the refractive-index difference can be achieved by choosing two different materials for substrate and film. In a subsequent step, which will be described in the following section, the surface of the layer can be structured to achieve channel waveguides. If the unstructured or structured layer is overgrown by another layer of lower refractive index—often the substrate material again—buried planar or channel waveguide structures are obtained.

3.1. Liquid-phase epitaxy

Liquid-phase epitaxy (LPE) is a process in which a single-crystal layer is grown from a dilute molten solution onto a flat, oriented single-crystal substrate. Epitaxy can be classified into homoepitaxy, when layer and substrate have the same chemical composition and crystal structure, and heteroepitaxy, in which layer and substrate are different in their chemical compositions but similar in their crystallographic relations. Most waveguiding layers grown by LPE can be considered as almost homoepitaxial, because they differ from the substrate only by the presence of a small amount of doping ions [1]. Historically, LPE has been the pioneering technology for preparing epitaxial layers of compound semiconductors, mainly III–V materials, like GaAs, GaSb, InP, and their ternary alloys [2]. In 1972, the first LPE experiments on transparent optical materials showed that high-quality layers can be successfully produced for applications such as waveguide lasers, amplifiers, and saturable absorbers [3].

Fig. 3 shows schematically an experimental LPE set-up, based on a resistance-heated furnace with vertical loading. Inside the furnace, there is a crucible filled with a molten solution. The solution contains the layer constituents dissolved in an appropriate solvent. When cooling the liquid solution down, at a certain temperature it becomes supersaturated. The substrate, which is often a polished single crystal, is immersed and rotated in the supersaturated solution, and the desired layer can be grown. After the growth, the substrate with layer is withdrawn from the liquid and the whole system is cooled down to room temperature [4,5]. If a suitable mask is deposited on the substrate before the growth process, even optical channel waveguides can be grown directly on the substrate [6].

The major advantage of LPE compared to epitaxial techniques from the vapor phase is that LPE is a near-thermodynamic equilibrium process, since supersaturations imposed for the growth are very low. Thus, single-

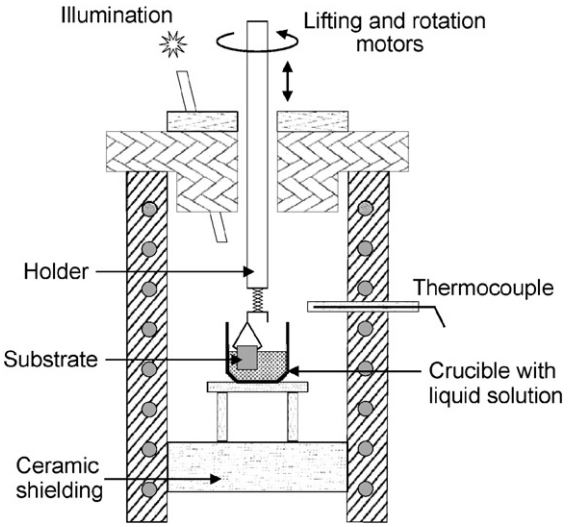

Fig. 3. Experimental set-up for LPE with vertical dipping of the substrate.

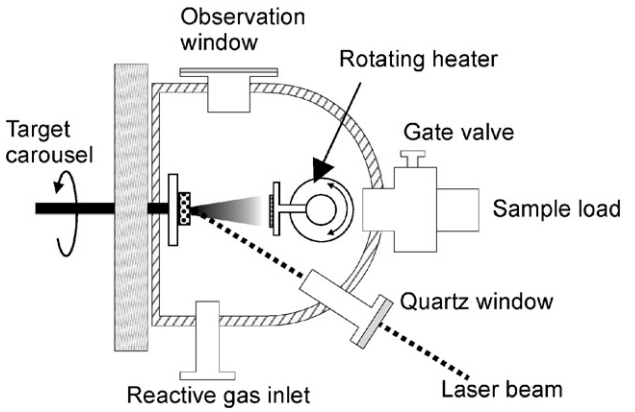

Fig. 4. Schematic diagram of a PLD system.

crystalline layers with thickness from 1 to 100 μm are feasible. The high crystalline quality of LPE-grown layers results in waveguide propagation losses as low as 0.05 dB/cm for a YAG:Nd waveguide [7]. In addition, LPE is a non-vacuum process, thus a low-cost and simple apparatus is used. The most notable limitations of LPE are poor uniformity of the layer surface and problems to grow a large number of uniformly stacked layers.

3.2. Pulsed laser deposition

Pulsed laser deposition (PLD) is one of the most popular and versatile techniques used for deposition of thin films. Although significant development of this method began only in the late 1980s, PLD is now widely used, particularly in oxide research.

In this method, a pulsed laser is directed onto a solid target, which is located in a vacuum chamber (Fig. 4). The most attractive laser sources are excimer lasers operating at 193, 248, or 308 nm wavelength, which ensure short pulse duration, high energy density, and high absorbance by most target materials. The nanosecond laser pulse is focused to provide an energy density sufficient to vaporize a few tens of nanometers of surface material in the form of neutral or ionic atoms and molecules with kinetic energies of a few eV. The ablated material is ejected from the target in a forward-directed plume. The ablation plume provides the material flux for layer deposition onto the substrate. A background gas is often introduced which serves two purposes. First, the formation of an oxide film requires oxidizing species (typically molecular oxygen) as a component of the flux. Second, the gas can be used to reduce the kinetic energies of the high-energy ablated species which may create defects in the growing film.

PLD has several attractive features, including the capability for stoichiometric transfer of material from target to substrate and easy control of the layer thickness in real time by turning the laser on and off. Since the laser is used as an external energy source, the deposition is an extremely clean process without filaments. Finally, the use of a carousel, housing a number of target materials, enables multi-layer stacks to be deposited without the need to break vacuum when changing between different materials.

The main drawback of PLD is its far-from-equilibrium nature of deposition. The ablated material contains macroscopic particulates up to 1 μm in diameter. The incorporation of these particulates into the film is detrimental to its optical properties. When depositing layers of complex oxides, the formation of thermodynamically stable binary oxides and other parasitic phases often occurs, e.g., during the PLD of $KGd(WO_4)_2$:Nd layers [8]. As listed in a review of PLD-grown oxides [9], most layers possess a thickness of only 0.5–1 μm and are polycrystalline. Therefore, propagation losses of PLD-developed waveguides are higher than those fabricated by LPE or ion in-diffusion, typically 1–5 dB/cm.

3.3. Thermal bonding

Thermal bonding is a new promising method for the fabrication of oxide layers, in particular for applications as high-power planar waveguide lasers [10]. This technique involves the assembly by optical contacting of precision-finished crystal or glass components and subsequent thermal treatment to increase the bonding strength. If thermal treatment does not proceed up to temperatures where interdiffusion between adjacent polished surfaces occurs, a wide variety of dissimilar materials may be bonded without formation of significant stress. Van-der-Waals intermolecular attractive forces are thought to be responsible for holding the individual components together.

Since thermal bonding does not require any bonding agents, reflections at interfaces are mainly due to the differences in refractive indices between the components, i.e., optical waveguiding is possible. For instance, laser operation from a side-pumped YAG:Yb planar waveguide prepared by thermal bonding on a YAG substrate has been reported [11]. A series of Nd-doped thermally bonded garnet layers were tested as waveguide lasers, and propagation losses, inferred from the laser performance, were from 0.4 to 0.7 dB/cm [10]. The scattering loss is mainly due to the imperfections in the optical surfaces of the individual components and possibly subsurface damage.

The main difficulty in thermal bonding is the thorough preparation of the substrate surface which should be atomically flat without any inclusions over the whole substrate area, otherwise the bonding will not be efficient.

4. Channel waveguide fabrication by surface structuring

Different physical or chemical methods for surface structuring of thin layers have been explored in the past. For the purpose of channel waveguide fabrication, it is important to achieve very low surface and sidewall roughness in the range of a few nanometers in order to keep the additional scattering losses introduced by the channel structure at a minimum.

4.1. Reactive ion etching and ion beam etching

Reactive ion etching (RIE) is a well-established method for patterning semiconductor materials. Especially in Si-based materials, deep etching of sub-μm structures with very high accuracy is achieved due to the chemical component of the process and special side-wall ceiling processes during etching. When etching dielectric crystalline solids by RIE, the physical component of the etching process is usually dominant, which often results in low etch rates in the range of 50 nm/min and rather unfortunate sample/mask etch ratios, because usually the mask consists of softer material than the crystalline sample. In addition, the obtained structures are often limited to the μm range, because deep etching processes have as yet not been developed for dielectric crystalline solids. Nevertheless, even under these conditions, careful choice of mask material and mask preparation in combination with adjustment of the etch parameters, such as gas composition and pressure as well as inductive power, leads to satisfactory results in the fabrication of rib channel waveguides with dimensions of typically several micrometer height and width in many crystalline materials. Although it is generally difficult to control the angle of the sidewall with respect to the film plane, the obtained sidewall smoothness and low surface roughness of a few nanometers ensures good waveguiding properties with low surface scattering losses.

Fig. 5(a) shows a flow-chart of the process of reactive ion etching. The waveguide surface is etched through an appropriate mask. As an example, a RIE-etched Ti:sapphire rib channel waveguide is displayed in Fig. 5(b). The process for the RIE of (Ti-doped) sapphire uses chlorine atmosphere, because aluminum ions (from Al_2O_3) react chemically with chloride ions, thereby forming rather volatile $AlCl_3$ molecules, which are easily removed from the sample surface. Detailed reports can be found in [13–16].

4.2. Ion beam implantation and wet chemical etching

Wet chemical etching is another, often employed method for surface structuring. Although wet chemical etching is usually an isotropic process, it can be non-isotropic in crystalline structures because of the different etch speeds along distinct crystal directions. However, a number of hard crystalline materials are chemically inert to the usually employed chemical agents. Specific chemical agents that are capable of etching such materials with reasonable speed may etch the employed mask material even faster.

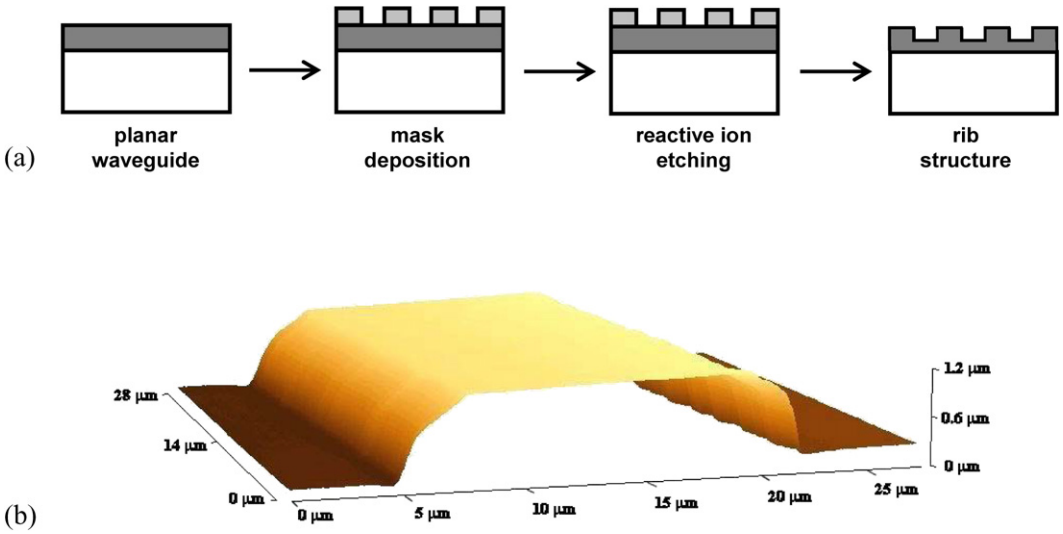

Fig. 5. (a) Flow chart of a reactive ion etching process; (b) atomic-force-microscope image of a Ti:sapphire rib channel waveguide profile. Figures taken from [12] and [13], respectively.

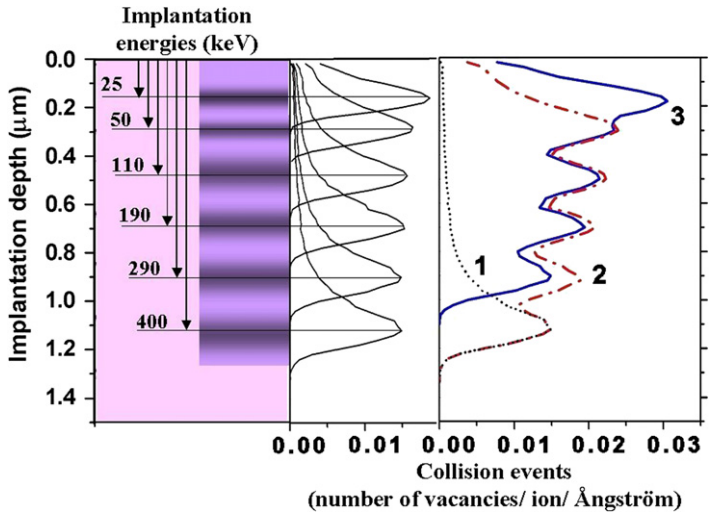

Fig. 6. Simulated (left-hand side) and accumulated (right-hand side) damage profiles of ion-beam implanted sapphire section generated by He^+ ions with different energies for subsequent wet chemical etching. Figure taken from [17].

In order to increase the etch rate of crystalline materials and improve the selectivity of the wet etching process, one can choose to damage the material prior to wet etching by ion implantation. Most of the radiation damage is generated at the end of the ions' tracks, at a depth proportional to the ions' energy. Such buried damaged layers are not attacked by the etchant. For complete etching from the surface, several ion energies must be employed that assure an almost continuous damage profile up to the crystal surface. When implanting ions through masks and varying the implantation energy and dose, very specific—even three-dimensional—damage patterns may be obtained.

As an example, we show the implantation profiles obtained by multiple-energy implantation of sapphire by He^+ ions (Fig. 6). The etching of sapphire by subsequent wet chemical etching is based on the fact that crystalline sapphire is extremely resistant to most chemical agents, whereas amorphous or ion-damaged Al_2O_3 can be attacked by different acidic solutions [18–21]. Ion beam implantation of sapphire produces damage clusters and, depending on ion type, dose and energy, even amorphization of implanted regions [18,19,22,23]. Early studies on etching ion-implanted sapphire were limited to the use of heavy ions and toxic (HF containing) acidic solutions, allowing for the structuring

of sapphire with depths of only a few hundreds of nanometers [24,25]. Using lighter He ions with energies up to 400 keV and hot H_3PO_4 as the etchant [26] allows for etch depths larger than 1 μm [17]. In this way, rib channel waveguides can be obtained in Ti:sapphire thin films.

4.3. Laser ablation

Laser ablation has been investigated by use of nanosecond pulses from excimer or Q-switched solid-state lasers as well as femtosecond pulses from mode-locked solid-state lasers. Both forms of pulsed optical energy are generally capable of ablating material from any crystalline surface up to several μm in depth. Typically, the resulting structures are by far not as well controlled as those obtained with the previously mentioned methods. Especially the rather large sidewall roughness would introduce high scattering losses to optical channel waveguides. It is also not possible with laser ablation to reach similarly tiny structure scales down to a few μm as with the previously mentioned methods. In addition, the re-deposition of ablated material in the rib region can pose a problem to the fabrication process, although different procedures to overcome this problem have been demonstrated. It can be concluded that laser ablation is currently not a suitable method for the fabrication of low-propagation-loss channel waveguides.

5. Waveguide fabrication by refractive-index variation

Since the deposition of thin optical layers is usually a time-consuming process which requires special equipment and precise adjustment of growth parameters, yet may lead to unsatisfactory results concerning layer and interface quality, alternative methods for optical waveguide fabrication without the need for thin-layer deposition have been investigated. The most successful approaches are ion in-diffusion, proton exchange, ion beam implantation, and direct laser writing. These methods, which shall be reviewed in this section, rely on the modification of bulk material properties by adding or exchanging ions or restructuring the material, in all cases resulting in a change of refractive index. Depending on the method as well as the treated material, this refractive-index change can be positive or negative, requiring different strategies for waveguide formation: In the former case the modified region itself forms the waveguide, in the latter case it serves as a low-index barrier which confines an unmodified waveguide region. Since the modified region often exhibits increased scattering losses, the latter method has undoubtedly a great advantage, which unfortunately may be counter-balanced by the fact that only a refractive-index barrier rather than a step is created, therefore leading to radiation losses by light tunneling through the barrier.

Most of these methods are appropriate for glasses. Ion exchange followed by a field-assisted burial step [27] was demonstrated in glass substrates containing high concentrations of alkali ions. UV writing techniques, also in combination with bonding [28], necessitate photosensitive material. Femtosecond laser irradiation [29] and focused ion beam implantation (IBI) [30,31] allow for direct writing of buried channel waveguides in amorphous materials, because a positive refractive index change is induced in the modified regions. These methods have been investigated also for crystalline materials.

5.1. Ion in-diffusion

Thermal in-diffusion has been extensively used as a standard method for waveguide fabrication in $LiNbO_3$ [32], although it can be successfully applied for fabricating active and passive waveguide structures also in other important oxides, like sapphire [33]. The increase of refractive index in the waveguide region is achieved by in-diffusion of ions with higher polarizability, e.g., transition-metal ions. Optically inert ions can be in-diffused into an optically active bulk material solely for the purpose of defining the waveguide region in the active material. Alternatively, the in-diffusion of transition-metal or rare-earth ions leads to localized active gain regions in such waveguides.

The process of ion in-diffusion consists of two steps: First, a uniform planar metal layer with thickness 30–60 nm is deposited on the substrate surface. The layer can be structured with standard lithographic techniques to produce aligned metal strips. Second, high-temperature annealing is performed to diffuse the deposited ions into the substrate. The annealing temperature and time depend on the diffusion coefficient of the doping ion in the substrate material and can vary from 1000 °C for Ti in-diffusion into $LiNbO_3$ [32] to 1950 °C into sapphire [33].

The in-depth concentration profile of the in-diffused ions is usually close to a Gaussian distribution, and the refractive index changes linearly with doping concentration for most materials. For instance, Fig. 7 shows the con-

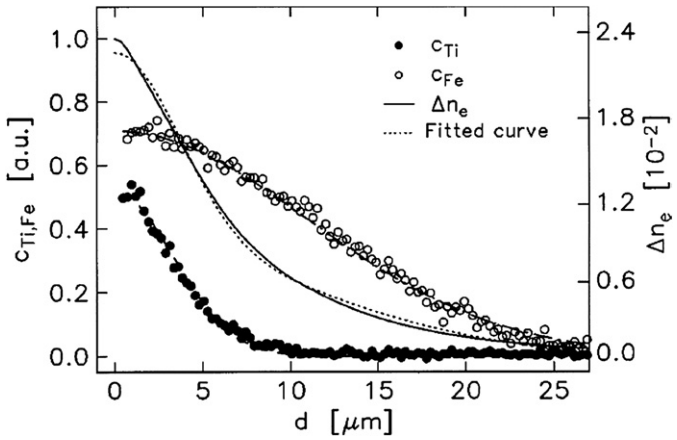

Fig. 7. Concentration profiles C_{Ti}, C_{Fe}, and reconstructed extraordinary refractive-index profile Δn_e of a planar $LiNbO_3$:Ti:Fe waveguide fabricated by ion in-diffusion. Figure taken from [34].

centration profiles of titanium, iron, and reconstructed extraordinary refractive-index profile of a planar $LiNbO_3$:Ti:Fe waveguide [34]. The refractive-index profile (solid line) can be approximated by a linear superposition (dotted line) of the iron and titanium concentration profiles.

A great advantage of the ion in-diffusion technique is the easy fabrication of various channel waveguides with desired geometries. However, the refractive-index change is always graded in both the vertical and horizontal directions. Propagation losses of in-diffused channel waveguides are typically 0.1–1 dB/cm [35].

5.2. Proton exchange

Exchange of one structure-constituting ion by another modifies the refractive index and has been attempted for several materials. Proton exchange, in particular, is a low-temperature process ($T < 250\,^{\circ}C$), which has been employed successfully for waveguide fabrication in $LiNbO_3$ and $LiTaO_3$. The substrate is masked to expose the areas, which are to be transformed into waveguiding regions, and immersed in a heated acid bath. The hydrogen ions diffuse into the substrate and exchange with lithium ions in the $LiNbO_3$ structure. The lithium ions diffuse out of the structure. As a result, the new chemical composition $Li_{1-x}H_xNbO_3$ is formed at a surface depth of 1–10 μm. A bath of a molten benzoic [36], phosphoric [37], or sulfuric [38] acid is used as the proton source. For deep proton penetration, the substrate can be exposed to the vapor of organic acid (so-called vapor-phase proton exchange). The lattice disorder and mixture of the different phases present in strongly exchanged layers, which can result in a significant degradation of electro-optical and non-linear properties of waveguides, can be removed during post-annealing at 300–350 °C [39].

The presence of protons in the sample results in a decreased ordinary and increased (up to 0.145 in $LiNbO_3$ [37]) extraordinary refractive index, so that optical waveguiding may be accomplished [40]. Deep proton exchange following titanium in-diffusion creates waveguides which support both polarizations. Because of the low-temperature fabrication, integrated devices are readily fabricated by masking the surface during exchange. $LiNbO_3$ channel waveguides fabricated with pure benzoic acid have typical propagation losses between 0.5 and 1 dB/cm.

5.3. Ion beam implantation

Ion beam implantation (IBI) was already mentioned in Section 4.2 in connection with subsequent wet chemical etching of the areas damaged by the implanted ions. Here, direct refractive index modifications as a result of IBI, possibly followed by post-implantation annealing, are of interest. Implantation of crystalline matrices often produces negative refractive index changes [22,41], although positive index changes induced by IBI have been observed in a few crystalline materials, such as $LiNbO_3$ [42], $KNbO_3$ [43], and YAG:Nd^{3+} [44].

The fact that negative refractive index changes are obtained by IBI in many crystalline materials leads to a large design flexibility in waveguide fabrication [41]. Surface and buried, planar as well as channel waveguides can be fabricated in hard crystalline materials by high-energy light-ion implantation. Good control of the implantation

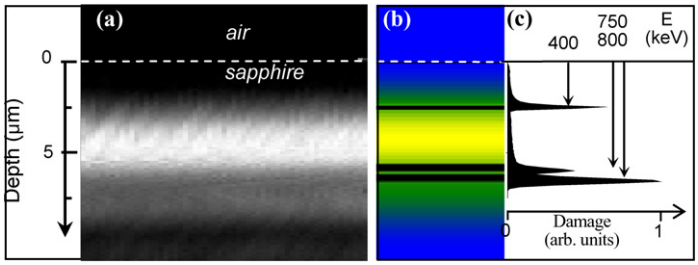

Fig. 8. Ion-beam implanted sapphire buried planar waveguide. (a) Experimental output profile of end-coupled 780-nm fundamental-mode laser light, (b) simulated contour plot, and (c) calculated accumulated damage profiles in sapphire. Figure taken from [41].

parameters, namely ion energy and dose, enables writing of precisely localized optical barriers with well-defined decrease of refractive index and provides excellent confinement of the guided light in each structure. In combination with contact masks, also side-barriers for the fabrication of channel waveguides can be produced. Low propagation losses—e.g., 0.7 dB/cm in sapphire [41]—can be obtained in fundamental-mode, buried channel waveguides without post-implantation annealing. Choice of the implantation parameters allows one to design mode shapes with different ellipticity and/or mode asymmetry in each orthogonal direction, thus demonstrating the versatility of the fabrication method. Horizontal and vertical parallelization for the design of one- or two-dimensional waveguide arrays is possible. Vertical stacking of buried waveguides is ultimately limited by the ion energy available from the Van-de-Graaf accelerator.

The choice of implanted ion is critical, as can be seen from the example of sapphire. Compared to the significant damage created in sapphire by He^+ implantation [17], which can be exploited for subsequent wet chemical etching (see Section 4.2) but results in poor waveguiding quality [45], protons create less damage in the guiding region, thus assuring better waveguiding quality. Moreover, deeper damage profiles are obtained with protons, for the same incident energy, thus providing larger design flexibility. An example of a buried planar waveguide in sapphire is shown in Fig. 8. In contrast, He^+ implantation was found to be superior to proton implantation in $KY(WO_4)_2$ mainly because of the high electronic damage produced by protons in the penetrated waveguiding region [46].

5.4. Femtosecond laser writing

Successful attempts to modify the refractive index of a material by irradiation with light have been made, e.g., with continuous-wave ultraviolet (UV) and femtosecond lasers. While UV light induces refractive index changes in glasses, such effects do usually not occur in hard crystalline materials. Nonlinear absorption of femtosecond laser pulses has been employed in order to induce structural changes by micro-explosions in numerous materials [47] and also for fabricating waveguide structures [29,48–50]. Femtosecond pulses can be used for precise micro-machining of materials, as the pulse energy is transferred to electrons and the optical excitation ends before the lattice is perturbed. The energy deposition is based on multiphoton absorption and avalanche ionization. The nonlinearity of the process can be exploited in order to write structures into the bulk of materials. Therefore, femtosecond writing provides the possibility of implementing three-dimensional optical integrated circuits. Another advantage of this fabrication process is the capability of rapid prototyping of a device without the need for any photolithographic process.

Whereas melting and re-solidification of glasses can be achieved with rather low pulse energies and typically results in positive refractive index changes, hard crystalline materials exhibit much higher damage thresholds and often negative refractive index changes. The damage threshold may be decreased and the writing process facilitated by appropriate sensitization of the material [50]. In principle, channel waveguides can be obtained by confining a waveguiding region between irradiated regions which form a low-refractive-index barrier, as in the example of ion beam implantation (Section 5.3). Alternatively, waveguiding can be obtained via a stress-induced refractive index increase in the vicinity of micro-damaged areas induced by femtosecond irradiation. However, such processes are currently not well understood, nor experimentally controllable. Hence, also the waveguide propagation losses are rather high, in the order of 2–4 dB/cm [50].

6. Examples of crystalline waveguide lasers

Among solid-state lasers, planar and especially channel waveguide lasers are characterized by lower laser thresholds than their bulk counterparts due to the confinement and excellent overlap between the laser and pump modes. This statement holds true provided that the waveguide fabrication process is well controlled and waveguide propagation losses are low. Channel geometries are particularly interesting due to their high brightness and capability of providing a fully diffraction-limited, near circular, fundamental-mode beam. This feature also makes them suitable for low-loss coupling with components such as optical fibers. Due to their compactness, waveguide lasers are becoming increasingly important as light sources in integrated optics.

Without aiming for completeness, some important recent results in the field of rare-earth-ion and transition-metal-ion doped oxide crystalline waveguide lasers are listed in Table 1. An overview of results published before 2003 can be found in [35]. In the following, we will highlight laser results obtained with crystalline waveguides fabricated by the aforementioned methods in sapphire, garnets, perovskites, double tungstates, and lithium niobate.

6.1. Ti:sapphire

Ti:sapphire is particularly attractive as a laser medium, because it offers a widely tunable laser output (650–1100 nm) [64], which can also be exploited for ultrashort-pulse generation with pulse durations of a few femtoseconds [65], and as a broadband light source in optical coherence tomography (OCT) for the investigation of biotissue [66,67].

Several methods have been investigated to fabricate Ti:sapphire planar waveguides, such as pulsed laser deposition [68–70], Ti^{3+} indiffusion in sapphire [33], and ion implantation [71,72]. In pulsed laser deposition (PLD), control of the valence state of the incorporated titanium dopant in the layer is of particular importance in order to avoid adverse effects such as parasitic absorption and subsequent limitations in the waveguide laser performance due to the presence of tetravalent titanium (Ti^{4+}) [70]. Laser oscillation was successfully demonstrated in Ti:sapphire planar waveguides fabricated by PLD on undoped sapphire substrates [73]. Recently, these Ti:sapphire waveguides have also demonstrated their suitability as broadband luminescence sources, and output powers sufficient to be considered for integration in existing OCT interferometric set-ups have been obtained [74].

Table 1
Examples of oxide crystalline waveguide lasers reported since 2003

Active material	Type of waveguide	Fabrication method	Laser wavelength (nm)	Threshold (mW)	Output power (mW)	Slope efficiency (%)	Ref.
Al_2O_3:Ti	channel	In-diffusion	775–821	210	0.25	0.11	[51]
Al_2O_3:Ti	channel	PLD + ion beam etching	792.5	265	27	5.3	[52]
Al_2O_3:Ti	channel	Ion beam implantation	778–783	380	17	3	[53]
Ta_2O_5:Nd	channel	Magnetron sputtering + reactive-ion-etching	1066	2.7	70	21	[54]
			1375	298	–	–	
$Y_3Al_5O_{12}$:Nd	channel	Femtosecond writing	1064	30	170	11	[55]
$Y_3Al_5O_{12}$:Nd	planar	Diffusion bonding	946	–	3500	57	[56]
			1064	–	4300	58	
			1318	–	2700	36	
			1833	300	400	7	
$Y_3Al_5O_{12}$:Nd	planar	Diffusion bonding	1064	$\sim 20 \times 10^3$	150×10^3	35	[57]
$Gd_3Ga_5O_{12}$:Nd	planar	PLD	1060.6	18	15	17.5	[58]
$KY(WO_4)_2$:Yb	planar	LPE	1024	80	290	80.4	[59]
$LiNbO_3$:Nd:Zn	channel	In-diffusion	1373.8	64	0.10	0.5	[60]
			1084.8	10.5	0.12	3	
$LiNbO_3$:Tm:Zn	channel	In-diffusion	1762.6	40	0.06	1	[61]
$LiNbO_3$:Ti:Fe:Er	channel	In-diffusion	1531.35	–	1.12	~0.5	[62]
$LiNbO_3$:Yb	channel	In-diffusion + proton exchange	1061	40	1.2×10^{-3}	3×10^{-3}	[63]

Due to its excellent thermal, mechanical, and optical properties, sapphire is one of the most suitable materials for integrated optical devices. Although this hard crystalline material is particularly difficult to process, surface channel waveguides in sapphire and Ti:sapphire have been obtained by a number of methods that require the use of photolithographic masks, such as rib fabrication by reactive ion etching [13] or Ar-ion milling [75] of Ti:sapphire planar waveguides, ion implantation and subsequent wet chemical etching [17,21], localized Ti^{3+} in-diffusion of sapphire [33], and alteration of the refractive index of Ti:sapphire planar waveguides by in-diffusion of Ga ions [76]. Also exploitation of a thin-film-induced photo-elastic effect [77] and laser ablation [12,78] has been investigated. Laser operation has recently been obtained in Ti:sapphire rib channel waveguides with output powers up to 27 mW and a slope efficiency of 5% [52]. Such channel waveguides may also be suitable as an alternative to femtosecond lasers [79] as broadband light sources in OCT set-ups.

Buried channel waveguides with low propagation losses down to 0.7 dB/cm have been obtained by proton implantation [41] and the first Ti:sapphire buried channel waveguide laser has recently been demonstrated in such a proton-implanted structure [53]. Recently, also direct femtosecond laser writing of buried channel waveguides in Ti:sapphire has been reported, however with rather uncontrolled waveguide dimensions and high propagation losses of typically 2–4 dB/cm [50].

6.2. Garnets

Pulsed laser deposition (PLD) has been proven a reliable technique for the growth of waveguiding films of garnets. Lasing has so far been observed in PLD-grown $Gd_3Ga_5O_{12}$:Nd [80,81]. Recently, low-loss (0.1 dB/cm) films of this material could be grown and planar waveguide lasing with a pump threshold of 18 mW, laser output power of 15 mW, and slope efficiency of 17.5% was demonstrated [58].

$Y_3Al_5O_{12}$:Nd planar waveguides were fabricated by several methods, e.g., by diffusion bonding [57]. Laser output from planar waveguides was demonstrated at all the typical electronic transitions from the $^4F_{3/2}$ level in Nd^{3+} at 946, 1064, 1318, and 1833 nm with output powers in the range of typically several watts [56]. The highest output power reported to date is 150 W at 1064 nm with a slope efficiency of 35% [57]. Channel waveguides were fabricated by, e.g., femtosecond laser writing [55] and a laser output power of 170 mW and slope efficiency of 11% were achieved. This slope efficiency which is rather low for a Nd^{3+} laser at 1064 nm shows indeed that femtosecond laser writing produces channel waveguides in crystalline materials with rather high propagation losses (see Section 5.4).

6.3. $YAlO_3$

Similar to garnets, channel waveguide lasers can be obtained by use of ion beam implantation also in other important oxide crystals, like $YAlO_3$ (YAP) which has a distorted perovskite crystal structure. Laser operation in a YAP:Nd waveguide was reported in 1990 [82]. The planar waveguide was fabricated by implanting He^+ ions with a total dose of 4.5×10^{16} ions/cm^2. A low refractive-index barrier was formed at a depth of 4 μm and the waveguide length was 0.66 mm. The upper limit of the waveguide propagation loss was estimated to be 15 dB/cm at 610 nm. Reflective mirrors were directly butt-coupled with a fluorinated liquid onto the end-faces of the waveguide and laser operation at ∼1.07 μm was achieved under longitudinal pumping with a CW Rhodamine 6G dye laser at 590 nm. The laser threshold was 50 (84) mW versus absorbed (launched) pump power.

Several attempts have been made to fabricate YAP:Nd waveguides by PLD, see, e.g., [83]. Layers with 20 μm thickness were deposited on sapphire and YAP substrates. However, because of the layer amorphization and presence of impurity phases, like $Y_4Al_2O_9$, reproducible waveguide propagation was not possible.

6.4. Double tungstates

Monoclinic double tungstate crystals, $KMe^{III}(WO_4)_2$ (Me^{III} = Y, Gd, or Lu), doped with different rare-earth ions are recognized as very promising materials for solid-state lasers operating both in pulsed and continuous-wave mode. Their low laser threshold, high efficiency, and third-order non-linear effects have stimulated research towards miniaturized waveguide lasers and amplifiers.

The first thin-film growth of a double tungstate by PLD was reported in 2000 [8]. Laser ablation of a stoichiometric single-crystal target was employed to obtain thin films of $KGd(WO_4)_2$:Nd. The films were polycrystalline with a thickness of about 0.7 μm. However, the propagation losses of 5 dB/cm were too high for laser operation.

The first waveguide laser based on the monoclinic double tungstate was demonstrated in 2006 [59]. High-quality $KY(WO_4)_2$:Yb planar layers with thickness up to 100 μm were produced by LPE on $KY(WO_4)_2$ substrates. Continuous-wave (CW) lasing in both surface and buried $KY(WO_4)_2$:Yb planar waveguides was demonstrated at 1025 nm in the fundamental mode under longitudinal pumping with a Ti:sapphire laser at 980 nm. The maximum output power was 290 mW and the slope efficiency was as high as 80.4%, to the best of our knowledge the highest value ever reported for a planar waveguide laser. The propagation losses were in the range of 0.07–0.18 dB/cm.

Yb-doped waveguide lasers are interesting because of the simple two-level energy scheme of the Yb^{3+} ion, which excludes excited-state depopulation due to excited-state absorption or energy-transfer processes. Since a significant part of the ground-state Yb^{3+} population is thermally excited to the lower Stark laser level, employing a waveguide geometry provides efficient pumping of Yb^{3+} ions because of the high pump confinement in the waveguide.

Current work involves the demonstration of a $KY(WO_4)_2$:Tm planar waveguide laser [84] and methods for channel waveguide fabrication [85].

6.5. $LiNbO_3$

$LiNbO_3$ is of interest because of its nonlinear, electro-optic, and acousto-optic properties. Optically active, low-loss embedded waveguide strips can be fabricated by planar in-diffusion of rare-earth ions into $LiNbO_3$ and subsequent preparation of channel waveguides by selective in-diffusion of transition metal ions (Ti or Zn). Recently, $LiNbO_3$:Yb channel waveguides were also fabricated by annealed proton exchange using an Al film with channel openings [63].

A variety of advanced waveguide laser devices has been demonstrated in Nd, Er, Tm, or Yb-codoped $LiNbO_3$. A list of waveguide lasers reported until 2003 can be found in reviews [9,35], whereas Table 1 provides examples reported recently.

Doping of $LiNbO_3$ waveguides with Nd allows the fabrication of efficient waveguide lasers with laser thresholds as low as 3.5 mW for channel waveguides in $LiNbO_3$:Nd:Ti and 1.25 mW in $LiNbO_3$:Nd:Zn [35].

Er-doped $LiNbO_3$ waveguide lasers emitting in the wavelength range 1530–1603 nm are excellent multifunctional components for integrated optics. Free-running lasers of the Fabry–Perot and ring types, harmonically mode-locked lasers (5 ps, 10 GHz), Q-switched lasers (4 ns, 1 kHz, 1 kW), distributed Bragg-reflector (DBR) lasers, self-frequency doubling devices, and acousto-optically tunable lasers have been reported [86,87].

7. Conclusions

As has been shown in the preceding sections, in recent years a number of methods for the fabrication of crystalline waveguides, either starting from layer deposition or by direct refractive-index modification in bulk material, have been established. These efforts have led to many different types of waveguide structures, and various crystalline waveguide lasers have since been demonstrated. While the majority of these devices are employed as transverse fundamental-mode light sources, specifically in $LiNbO_3$ also the optical nonlinearity of the material has been exploited for applications in integrated optics. It can be foreseen than in the future also other crystalline materials will be used for further optical integration in order to achieve, e.g., tunable or ultrashort-pulse integrated lasers in Ti:sapphire or highly efficient light sources combined with other optical structures in high-refractive-index materials such as double tungstates. The large potential of gain in crystalline waveguide integrated structures may become more visible within the next several years.

References

[1] B. Ferrand, B. Chambaz, M. Couchaud, Liquid phase epitaxy: A versatile technique for the development of miniature optical components in single crystal dielectric media, Opt. Mater. 11 (1999) 101–114.

[2] H. Nelson, Epitaxial growth from the liquid state and its application to the fabrication of tunnel and laser diodes, RCA Rev. 24 (4) (1963) 603–615.

[3] P.K. Tien, R.J. Martin, S.L. Blank, S.H. Wemple, L.J. Varnerin, Optical waveguides in single-crystal garnet films, Appl. Phys. Lett. 21 (5) (1972) 207–209.

[4] D. Ehrentraut, M. Pollnau, S. Kück, Epitaxial growth and spectroscopic investigation of $BaSO_4:Mn^{6+}$ layers, Appl. Phys. B 75 (1) (2002) 59–62.
[5] Y.E. Romanyuk, I. Utke, D. Ehrentraut, V. Apostolopoulos, M. Pollnau, S. García-Revilla, R. Valiente, Low-temperature liquid phase epitaxy and optical waveguiding of rare-earth-ion doped $KY(WO_4)_2$ thin layers, J. Cryst. Growth 269 (2–4) (2004) 377–384.
[6] Y.E. Romanyuk, Liquid-phase epitaxy of doped $KY(WO_4)_2$ layers for waveguide lasers, Ph.D. Thesis, Ecole Polytechnique Fédérale de Lausanne, Switzerland, 2005.
[7] I. Chartier, B. Ferrand, D. Pelenc, S.J. Field, D.C. Hanna, A.C. Large, D.P. Shepherd, D.C. Tropper, Growth and low-threshold laser oscillation of an epitaxially grown Nd:YAG waveguide, Opt. Lett. 17 (11) (1992) 10–12.
[8] P.A. Atanasov, R.I. Tomov, J. Perriére, R.W. Eason, N. Vainos, A. Klini, A. Zherikhin, E. Millon, Growth of Nd:potassium gadolinium tungstate thin-film waveguides by pulsed laser deposition, Appl. Phys. Lett. 76 (18) (2000) 2490–2492.
[9] M. Jelinek, J. Lancok, J. Sonsky, J. Oswald, M. Simeckova, L. Jastrabik, V. Studnicka, Planar waveguide lasers and structures created by laser ablation—an overview, Czech. J. Phys. 48 (5) (1998) 577–597.
[10] C.T.A. Brown, C.L. Bonner, T.J. Warburton, D.P. Shepherd, A.C. Tropper, D.C. Hanna, H.E. Meissner, Thermally bonded planar waveguide lasers, Appl. Phys. Lett. 71 (9) (1997) 1139–1141.
[11] U. Griebner, R. Grunwald, H. Schönnagel, Thermally bonded Yb:YAG planar waveguide laser, Opt. Commun. 164 (4–6) (1999) 185–190.
[12] A. Crunteanu, P. Hoffmann, M. Pollnau, Ch. Buchal, A comparative study on methods to structure sapphire, Appl. Surf. Sci. 208–209 (2003) 322–326.
[13] A. Crunteanu, M. Pollnau, G. Jänchen, C. Hibert, P. Hoffmann, R.P. Salathé, R.W. Eason, C. Grivas, D.P. Shepherd, Ti:sapphire rib channel waveguide fabricated by reactive ion etching of a planar waveguide, Appl. Phys. B 75 (1) (2002) 15–17.
[14] J. Lančok, M. Jelínek, J. Bulíř, P. Macháč, Study of the fabrication of the channel waveguide in Ti:sapphire layers, Laser Phys. 8 (1) (1998) 303–306.
[15] Y.J. Sung, H.S. Kim, Y.H. Lee, J.W. Lee, S.H. Chae, Y.J. Park, G.Y. Yeom, High rate etching of sapphire wafer using $Cl_2/BCl_3/Ar$ inductively coupled plasmas, Mater. Sci. Eng. B 82 (1–3) (2001) 50–52.
[16] S.H. Park, H. Jeon, Y.J. Sung, G.Y. Yeom, Refractive sapphire microlenses fabricated by chlorine-based inductively coupled plasma etching, Appl. Opt. 40 (22) (2001) 3698–3702.
[17] A. Crunteanu, G. Jänchen, P. Hoffmann, M. Pollnau, Ch. Buchal, A. Petraru, R.W. Eason, D.P. Shepherd, Three-dimensional structuring of sapphire by sequential He^+ ion-beam implantation and wet chemical etching, Appl. Phys. A 76 (7) (2003) 1109–1112.
[18] C.W. White, C.J. McHargue, P.S. Skland, L.A. Boatner, G.C. Farlow, Ion implantation and annealing of crystalline oxides, Mater. Sci. Rep. 4 (2) (1989) 41–146.
[19] C.J. McHargue, J.D. Hunn, D.L. Joslin, E. Alves, M.F. da Silva, J.C. Soares, Etching of amorphous Al_2O_3 produced by ion implantation, Nucl. Instrum. Methods B 127–128 (1997) 596–598.
[20] P. Levy, S. Nicoletti, L. Correra, M. Cervera, M. Bianconi, F. Biscarini, F. Corticelli, E. Gabilli, Fabrication of step-edge structures on R-plane sapphire using a selective wet etch process, Nuovo Cimento D 19 (8–9) (1997) 1389–1395.
[21] D. Xie, D. Zhu, H. Pan, H. Xu, Z. Ren, Enhanced etching of sapphire damaged by ion implantation, J. Phys. D: Appl. Phys. 31 (14) (1998) 1647–1651.
[22] P.D. Townsend, P.J. Chandler, L. Zhang, in: P.L. Knight, A. Miller (Eds.), Optical Effects of Ion Implantation, Cambridge Univ. Press, Cambridge, 1994.
[23] Ch. Buchal, S.P. Withrow, C.W. White, D.B. Poker, Ion implantation of optical materials, Annu. Rev. Mater. Sci. 24 (1994) 125–157.
[24] M. Ishida, H. Kim, T. Kimura, T. Nakamura, A new etching method for single-crystal Al_2O_3 film on Si using Si ion implantation, Sensor Actuat. A-Phys. 53 (1–3) (1996) 340–344.
[25] F. Gonzalez, J.W. Halloran, Reaction of ortho-phosphoric acid with several forms of aluminum-oxide, Ceram. Bull. 59 (7) (1980) 727.
[26] E. Makino, T. Shibata, Y. Yamada, Micromachining of fine ceramics by photolithography, Sensor Actuat. A-Phys. 75 (3) (1999) 278–288.
[27] G. Jose, G. Sorbello, S. Taccheo, E. Cianci, V. Foglietti, P. Laporta, Active waveguide devices by Ag–Na ion exchange on erbium–ytterbium doped phosphate glasses, J. Non-Cryst. Solids 322 (1–3) (2003) 256–261.
[28] C.B.E. Gawith, A. Fu, T. Bhutta, P. Hua, D.P. Shepherd, E.R. Taylor, P.G.R. Smith, D. Milanese, M. Ferrarris, Direct-UV-written buried channel waveguide lasers in direct-bonded intersubstrate ion-exchanged neodymium-doped germano-borosilicate glass, Appl. Phys. Lett. 81 (19) (2002) 3522–3524.
[29] K.M. Davies, K. Miura, N. Sugimoto, K. Hirao, Writing waveguides in glass with a femtosecond laser, Opt. Lett. 21 (21) (1996) 1729–1731.
[30] A. Roberts, M.L. von Bibra, Fabrication of buried channel waveguides in fused silica using focused MeV proton beam irradiation, J. Lightwave Technol. 14 (11) (1996) 2554–2557.
[31] K. Liu, E.Y.B. Pun, T.C. Sum, A.A. Bettiol, J.A. van Kan, F. Watt, Erbium-doped waveguide amplifiers fabricated using focused proton beam writing, Appl. Phys. Lett. 84 (5) (2004) 684–686.
[32] R.V. Schmidt, I.P. Kaminow, Metal-diffused optical waveguides in $LiNbO_3$, Appl. Phys. Lett. 25 (8) (1974) 458–460.
[33] L.M.B. Hickey, J.S. Wilkinson, Titanium diffused waveguides in sapphire, Electron. Lett. 32 (24) (1996) 2238–2239.
[34] D. Kip, Photorefractive waveguides in oxide crystals: fabrication, properties, and applications, Appl. Phys. B 67 (2) (1998) 131–150.
[35] M. Jelinek, Progress in optical waveguiding thin films, Czech. J. Phys. 53 (5) (2003) 365–377.
[36] J.M. Cabrera, J. Olivares, M. Carrascosa, J. Rams, R. Müller, E. Dieguez, Hydrogen in lithium niobate, Adv. Phys. 45 (5) (1996) 349–392.
[37] K. Yamamoto, T. Taniuchi, Characteristics of pyrophosphoric acid proton-exchanged waveguides in $LiNbO_3$, J. Appl. Phys. 70 (11) (1991) 6663–6668.
[38] J.T. Cargo, A.J. Filo, M.C. Hughes, V.C. Kannan, F.A. Stevie, J.A. Taylor, J.R. Holmes, Characterization of sulfuric acid proton-exchanged lithium niobate, J. Appl. Phys. 67 (2) (1990) 627–633.
[39] P.G. Suchoski, T.K. Findakly, F.J. Leonberger, Stable low-loss proton-exchanged $LiNbO_3$ waveguide devices with no electro-optic degradation, Opt. Lett. 13 (11) (1988) 1050–1052.

[40] J. Jackel, A.M. Glass, G.E. Peterson, C.E. Rice, D.H. Olson, J.J. Veselka, Damaged-resistant $LiNbO_3$ waveguides, J. Appl. Phys. 55 (1) (1984) 269–270.
[41] L. Laversenne, P. Hoffmann, M. Pollnau, P. Moretti, J. Mugnier, Designable buried waveguides in sapphire by proton implantation, Appl. Phys. Lett. 85 (22) (2004) 5167–5169.
[42] J. Rams, J. Olivares, P.J. Chandler, P.D. Townsend, Mode gaps in the refractive index properties of low-dose ion-implanted $LiNbO_3$ waveguides, J. Appl. Phys. 87 (7) (2000) 3199–3202.
[43] F.P. Strohkendl, D. Fluck, P. Günter, R. Irmscher, Ch. Buchal, Nonleaky optical waveguides in $KNbO_3$ by ultralow dose MeV He ion implantation, Appl. Phys. Lett. 59 (26) (1991) 3354–3356.
[44] P. Moretti, M.F. Joubert, S. Tascu, B. Jacquier, M. Kaczkan, M. Malinowskii, J. Samecki, Luminescence of Nd^{3+} in proton or helium-implanted channel waveguides in Nd:YAG crystals, Opt. Mater. 24 (1–2) (2003) 315–319.
[45] P.D. Townsend, Optical waveguides formed by ion implantation in Al_2O_3 and $CaCO_3$, in: P. Mazzoldi (Ed.), Induced Defects in Insulators, in: MRS, vol. 207, Les Editions de Physique, Les Ulis, 1985, p. 207.
[46] C.N. Borca, F. Zäh, C. Schnider, R.P. Salathé, M. Pollnau, P. Moretti, Fabrication of optical planar waveguides in $KY(WO_4)_2$ by He-ion implantation, in: Conference on Lasers and Electro-Optics Europe, Munich, Germany, 2005, Conference Digest, paper CE6-3-FRI.
[47] E.N. Glezer, E. Mazur, Ultrafast-laser driven micro-explosions in transparent materials, Appl. Phys. Lett. 71 (7) (1997) 882–884.
[48] R. Osellame, S. Taccheo, M. Marangoni, R. Ramponi, P. Laporta, D. Polli, S. De Silvestri, G. Cerullo, Femtosecond writing of active optical waveguides with astigmatically shaped beams, J. Opt. Soc. Am. B 20 (7) (2003) 1559–1567.
[49] T. Gorelik, M. Will, S. Nolte, A. Tünnermann, U. Glatzel, Transmission electron microscopy studies of femtosecond laser induced modifications in quartz, Appl. Phys. A 76 (3) (2003) 309–311.
[50] V. Apostolopoulos, L. Laversenne, T. Colomb, C. Depeursinge, R.P. Salathé, M. Pollnau, R. Osellame, G. Cerullo, P. Laporta, Femtosecond-irradiation-induced refractive-index changes and channel waveguiding in bulk Ti^{3+}:sapphire, Appl. Phys. Lett. 85 (7) (2004) 1122–1124.
[51] L.M.B. Hickey, V. Apostolopoulos, R.W. Eason, J.S. Wilkinson, A.A. Anderson, Diffused Ti:sapphire channel-waveguide lasers, J. Opt. Soc. Am. B 21 (8) (2004) 1452–1456.
[52] C. Grivas, D.P. Shepherd, T.C. May-Smith, R.W. Eason, M. Pollnau, Single-transverse-mode Ti:sapphire rib waveguide laser, Opt. Express 13 (1) (2005) 210–215.
[53] L. Laversenne, C.N. Borca, M. Pollnau, P. Moretti, C. Grivas, D.P. Shepherd, R.W. Eason, Ti:sapphire buried channel waveguide laser by proton implantation, in: Conference on Lasers and Electro-Optics, Long Beach, California, 2006, Technical Digest, Optical Society of America, Washington, DC, 2006, paper JWB47.
[54] B. Unal, M.C. Netti, M.A. Hassan, P.J. Ayliffe, M.D.B. Charlton, F. Lahoz, N.M.B. Perney, D.P. Shepherd, C.Y. Tai, J.S. Wilkinson, G.J. Parker, Neodymium-doped tantalum pentoxide waveguide lasers, IEEE J. Quantum Electron. 41 (12) (2005) 1565–1573.
[55] A.G. Okhrimchuk, A.V. Shestakov, I. Khrushchev, J. Mitchell, Depressed cladding, buried waveguide laser formed in a YAG:Nd^{3+} crystal by femtosecond laser writing, Opt. Lett. 30 (17) (2005) 2248–2250.
[56] J.I. Mackenzie, C. Li, D.P. Shepherd, Multi-watt, high efficiency, diffraction-limited Nd:YAG planar waveguide laser, IEEE J. Quantum Electron. 39 (3) (2003) 493–500.
[57] J.R. Lee, H.J. Baker, G.J. Friel, G.J. Hilton, D.R. Hall, High-average-power Nd:YAG planar waveguide laser that is face pumped by 10 laser diode bars, Opt. Lett. 27 (7) (2002) 524–526.
[58] C. Grivas, T.C. May-Smith, D.P. Shepherd, R.W. Eason, Laser operation of a low loss (0.1 dB/cm) Nd:$Gd_3Ga_5O_{12}$ thick (40 μm) planar waveguide grown by pulsed laser deposition, Opt. Commun. 229 (1–6) (2004) 355–361.
[59] Y.E. Romanyuk, C.N. Borca, M. Pollnau, U. Griebner, S. Rivier, V. Petrov, Yb-doped $KY(WO_4)_2$ planar waveguide laser, Opt. Lett. 31 (1) (2006) 53–55.
[60] M. Domenech, G. Lifante, Continuous-wave laser operation at 1.3 μm in Nd^{3+}-doped Zn:$LiNbO_3$ channel waveguides, Appl. Phys. Lett. 84 (17) (2004) 3271–3273.
[61] E. Cantelar, J.A. Sanz-Garcia, G. Lifante, F. Cusso, P.L. Pernas, Single polarized Tm^{3+} laser in Zn-diffused $LiNbO_3$ channel waveguides, Appl. Phys. Lett. 86 (16) (2005) 161119.
[62] B.K. Das, R. Ricken, W. Sohler, Integrated optical distributed feedback laser with Ti:Fe:Er:$LiNbO_3$ waveguide, Appl. Phys. Lett. 82 (10) (2003) 1515–1517.
[63] M. Fujimura, H. Tsuchimoto, T. Suhara, Yb-diffused $LiNbO_3$ annealed/proton exchanged waveguide lasers, IEEE Photon. Technol. Lett. 17 (1) (2005) 130–132.
[64] P.F. Moulton, Spectroscopic and laser characteristics of Ti:Al_2O_3, J. Opt. Soc. Am. B 3 (1) (1986) 125–133.
[65] U. Morgner, F.X. Kärtner, S.H. Cho, Y. Chen, H.A. Haus, J.G. Fujimoto, E.P. Ippen, V. Scheuer, G. Angelow, T. Tschudi, Sub-two-cycle pulses from a Kerr-lens mode-locked Ti:sapphire laser, Opt. Lett. 24 (6) (1999) 411–413.
[66] M. Pollnau, Broadband luminescent materials in waveguide geometry, J. Lumin. 102–103 (2003) 797–801.
[67] A.M. Kowalevicz, T. Ko, I. Hartl, J.G. Fujimoto, M. Pollnau, R.P. Salathé, Ultrahigh resolution optical coherence tomography using a superluminescent light source, Opt. Express 10 (7) (2002) 349–353.
[68] P.E. Dyer, S.R. Jackson, P.H. Key, W.J. Metheringham, M.J.J. Schmidt, Excimer laser ablation and film deposition of Ti:sapphire, Appl. Surf. Sci. 96–98 (1996) 849–854.
[69] A.A. Anderson, R.W. Eason, M. Jelinek, C. Grivas, D. Lane, K. Rogers, L.M.B. Hickey, C. Fotakis, Growth of Ti:sapphire single crystal thin films by pulsed laser deposition, Thin Solid Films 300 (1–2) (1997) 68–71.
[70] P.R. Willmott, P. Manoravi, J.R. Huber, T. Greber, T.A. Murray, K. Holliday, Production and characterization of Ti:sapphire thin films grown by reactive laser ablation with elemental precursors, Opt. Lett. 24 (22) (1999) 1581–1583.
[71] P.D. Townsend, P.J. Chandler, R.A. Wood, L. Zhang, J. McCallum, C.W. McHargue, Chemically stabilised ion implanted waveguides in sapphire, Electron. Lett. 26 (15) (1990) 1193–1195.

[72] L.D. Morpeth, J.C. McCallum, Formation of Ti^{3+} in sapphire by co-implantation of Ti and O ions, Appl. Phys. Lett. 76 (4) (2000) 424–426.
[73] A.A. Anderson, R.W. Eason, L.M.B. Hickey, M. Jelinek, C. Grivas, D.S. Gill, N.A. Vainos, Ti:sapphire planar waveguide laser grown by pulsed laser deposition, Opt. Lett. 22 (20) (1997) 1556–1558.
[74] M. Pollnau, R.P. Salathé, T. Bhutta, D.P. Shepherd, R.W. Eason, Continuous-wave broadband emitter based on a transition-metal-ion-doped waveguide, Opt. Lett. 26 (5) (2001) 283–285.
[75] C. Grivas, D.P. Shepherd, T.C. May-Smith, R.W. Eason, M. Pollnau, A. Crunteanu, M. Jelinek, Performance of Ar^{+}-milled Ti:sapphire rib waveguides as single transverse mode broadband fluorescence sources, IEEE J. Quantum Electron. 39 (3) (2003) 501–507.
[76] V. Apostolopoulos, L.M.B. Hickey, D.A. Sager, J.S. Wilkinson, Gallium-diffused waveguides in sapphire, Opt. Lett. 26 (20) (2001) 1586–1588.
[77] M. Liu, H.K. Kim, Strain-induced channel waveguiding in bulk sapphire substrates, Appl. Phys. Lett. 79 (17) (2001) 2693–2695.
[78] A.J. Pedraza, Interaction of UV laser light with wide band gap materials: Mechanisms and effects, Nucl. Instrum. Methods B 141 (1–4) (1998) 709–718.
[79] W. Drexler, U. Morgner, F.X. Kärtner, C. Pitris, S.A. Boppart, X.D. Li, E.P. Ippen, J.G. Fujimoto, In vivo ultrahigh-resolution optical coherence tomography, Opt. Lett. 24 (17) (1999) 1221–1223.
[80] D.S. Gill, A.A. Anderson, R.W. Eason, T.J. Warburton, D.P. Shepherd, Laser operation of an Nd:$Gd_3Ga_5O_{12}$ thin-film optical waveguide fabricated by pulsed laser deposition, Appl. Phys. Lett. 69 (1) (1996) 10–12.
[81] C.L. Bonner, A.A. Anderson, R.W. Eason, D.P. Shepard, D.S. Gill, C. Grivas, N.A. Vainos, Performance of a low-loss pulsed-laser-deposited Nd:$Gd_3Ga_5O_{12}$ waveguide laser at 1.06 and 0.94 μm, Opt. Lett. 22 (13) (1997) 988–990.
[82] S.J. Field, D.C. Hanna, D.P. Shepherd, A.C. Tropper, P.J. Chandler, P.D. Townsend, L. Zhang, Ion-implanted Nd:YAP planar waveguide laser, Electron. Lett. 26 (21) (1990) 1826–1827.
[83] J. Sonsky, J. Lancok, M. Jelınek, J. Oswald, V. Studnicka, Growth of active Nd-doped YAP thin-film waveguides by laser ablation, Appl. Phys. A 66 (5) (1998) 583–586.
[84] S. Rivier, U. Griebner, V. Petrov, Y.E. Romanyuk, C.N. Borca, M. Pollnau, KYb$(WO_4)_2$:Tm^{3+} planar waveguide laser', 2006, submitted for publication.
[85] C.N. Borca, Y.E. Romanyuk, F. Gardillou, M. Pollnau, M.P. Bernal, P. Moretti, Optical channel waveguides in KY$(WO_4)_2$:Yb^{3+}, in: Conference on Lasers and Electro-Optics, Long Beach, California, 2006, Technical Digest, Optical Society of America, Washington, DC, 2006, paper CMFF3.
[86] W. Sohler, B.K. Das, D. Dey, S. Reza, H. Suche, R. Ricken, Erbium-doped lithium niobate waveguide lasers, IEICE Trans. Electron. E88-C (5) (2005) 990–997.
[87] C. Becker, T. Oesselke, J. Pandavenes, R. Ricken, K. Rochhausen, G. Schreiber, W. Sohler, H. Suche, R. Wessel, S. Balsamo, I. Montrosset, D. Sciancalepore, Advanced Ti:Er:$LiNbO_3$ waveguide lasers, IEEE J. Select. Topics Quantum Electron. 6 (1) (2000) 101–113.